OPEN ACCESS
IOP Publishing
Journal of Physics: Condensed Matter
J. Phys.: Condens. Matter **36** (2024) 145101 (9pp)
https://doi.org/10.1088/1361-648X/ad15c7

Active-parameter polydispersity in the 2d ABP Yukawa model

Shibu Saw, Lorenzo Costigliola and Jeppe C Dyre*

Glass and Time, IMFUFA, Department of Science and Environment, Roskilde University, PO Box 260, DK-4000 Roskilde, Denmark

E-mail: dyre@ruc.dk

Received 30 October 2023, revised 6 December 2023
Accepted for publication 14 December 2023
Published 4 January 2024

Abstract

In experiments and simulations of passive as well as active matter the most commonly studied kind of parameter polydispersity is that of varying particles size. This paper investigates by simulations the effects of introducing polydispersity in other parameters for two-dimensional active Brownian particles with Yukawa pair interactions. Polydispersity is studied separately in the translational and rotational diffusion coefficients, as well as in the swim velocity v_0. Uniform and binary parameter distributions are considered in the homogeneous and the motility-induced phase-separation (MIPS) phases. We find only minute changes in structure and dynamics upon the introduction of parameter polydispersity, even for situations involving 50% polydispersity. The reason for this is not clear. An exception is the case of v_0 polydispersity for which the average radial distribution function with changing polydispersity shows significant variations in the MIPS phase. Even in this case, however, the dynamics is only modestly affected. As a possible application of our findings, we suggest that a temporary introduction of polydispersity into a single-component active-matter model characterized by a very long equilibration time, i.e. a glass-forming active system, may be used to equilibrate the system efficiently by particle swaps.

Keywords: active Brownian particles, parameter polydispersity, structure and dynamics of active matter

1. Introduction

Active matter includes fluids of self-propelled particles like bacteria, birds, or insect flocks [1–7]. An example of the intriguing features of active matter is motility-induced phase separation (MIPS), the fact that a purely repulsive system may phase separate into high- and low-density phases [4, 8–12].

There is currently a considerable interest in passive polydisperse systems, in particular deriving from the use of polydispersity for SWAP-equilibrating models of supercooled liquids [13]. An obvious question that arises is: how different are the dynamics of the different particles [14–16]? Polydispersity is also relevant for biological systems in which one cannot expect all constituents to be identical [17–20]. Active-matter models with motility polydispersity have been studied in both biological and colloidal systems; thus de Castro *et al* recently showed that the MIPS phase gets suppressed with the introduction of a spread of swim (self-propelled) velocities in the active Brownian particles (ABP) model [21].

This paper presents a systematic study of the effects of polydispersity in other parameters than size [22, 23] of the ABP model in two dimensions. The particles interact via

* Author to whom any correspondence should be addressed.

the Yukawa (screened Coulomb) pair potential [24, 25], and polydispersity is introduced by varying the three activity parameters controlling the particle motion. We find a surprisingly small effect of even quite high polydispersity, up to 50%, when parameters vary such that their average is kept constant. This applies to both continuous and binary polydispersity and is in sharp contrast to the large effects of size polydispersity [22, 23].

2. The 2d ABP Yukawa system

The Yukawa pair potential [24, 26] is defined [27] by

$$v(r) = \frac{Q^2\sigma}{r}\exp\left(-\frac{r}{\lambda\sigma}\right). \tag{1}$$

Here σ is a length parameter, λ is dimensionless, and the 'charge' Q has dimension square root of energy. Throughout the paper we use $\lambda = 0.16$ and $Q = 50$, while $\sigma \equiv 1$ defines the unit of length and thus that of particle density.

If $\mathbf{r}_i$ is the position vector of particle i, the ABP equations of motion in two dimensions are [28]

$$\dot{\mathbf{r}}_i = \mu\mathbf{F}_i + \boldsymbol{\xi}_i(t) + v_0\,\mathbf{n}_i(t). \tag{2}$$

Here, μ is the mobility (velocity over force), $\mathbf{F}_i(\mathbf{R}) = -\nabla_i U(\mathbf{R})$ is the force on particle i in which $\mathbf{R} = (\mathbf{r}_1, \ldots, \mathbf{r}_N)$ is the configuration vector and $U(\mathbf{R}) = \sum_{i<j} v(r_{ij})$ (sum over all particle pairs) is the potential-energy function, $\boldsymbol{\xi}_i(t)$ is a Gaussian random white-noise vector, and v_0 is the swim velocity. The vector $\mathbf{n}_i(t) = (\cos\theta_i(t), \sin\theta_i(t))$ is a stochastic unit vector in which the angle $\theta_i(t)$ is controlled by a Gaussian white noise term the magnitude of which defines the rotational diffusion coefficient, D_r, according to

$$\langle\dot{\theta}_i(t)\,\dot{\theta}_j(t')\rangle = 2D_r\delta_{ij}\,\delta(t-t'). \tag{3}$$

The magnitude of the white-noise velocity vector $\boldsymbol{\xi}_i(t)$ defines the translational diffusion coefficient D_t,

$$\langle\boldsymbol{\xi}_i^{\alpha}(t)\,\boldsymbol{\xi}_j^{\beta}(t')\rangle = 2D_t\delta_{ij}\delta_{\alpha\beta}\delta(t-t') \tag{4}$$

in which α, β are spatial x, y indices. The mobility μ is taken to be unity throughout, i.e. μ is regarded as a material constant, while the remaining model parameters D_r, D_t, and v_0 are allowed to vary from particle to particle. This introduces three kinds of polydispersity. In all cases considered below the average of the polydisperse parameter in question is kept constant. For any varying parameter X, the polydispersity δ is conventionally defined [29] as $\delta \equiv \sqrt{\langle X^2\rangle - \langle X\rangle^2}/\langle X\rangle$ in which the sharp brackets denote averages.

We simulated 10 000 particles of the 2d Yukawa system with interactions cut off at 4.5σ. The time step used was $\Delta t = 0.0625\langle D_t\rangle/\langle v_0\rangle^2$. Each simulation involved $2\cdot 10^7$ time steps. The (GPU) code employed was RUMD [30], modified to deal with polydispersity in particle-activity parameters. Parameters corresponding to both the homogeneous phase ($D_t = 1.0$, $D_r = 0.8$, $v_0 = 25$) and the MIPS phase ($D_t = 1.0$, $D_r = 0.2$, $v_0 = 25$) were simulated.

3. Polydispersity in the homogeneous phase

We first consider the effect of active-parameter polydispersity on the structure and dynamics in the homogeneous phase. Figures 1(a), (c) and (e) show the (average) radial distribution functions (RDFs) for different degrees of polydispersity: uniform parameter distributions of 10% and 50% polydispersity and binary parameter distributions of 10%, 30%, and 50% polydispersity in D_t, (a) and (b), D_r, (c) and (d) and v_0, (e) and (f); in the figure x_A denotes the large-parameter fraction of particles.

Figures 1(b), (d) and (f) show the average mean-square displacement (MSD) as a function of time for the same situations. We find here the well-known three regimes [31]: diffusive (small time), ballistic (intermediate time), and diffusive (long time). The first regime is governed by the thermal noise, the second by the swim velocity, and the third by the rotational diffusion coefficient and swim velocity. There is little effect of polydispersity. This is not trivial because the individual particles conform to different equations of motion; indeed they move differently as becomes clear from the next figure.

To illuminate the role of parameter polydispersity for the individual particles, we identified for the two uniform polydispersities the particles with the 20% smallest activity parameters and those with the 20% largest. For each of these categories we determined the corresponding RDFs (counting only surrounding particles of the same type) and MSDs. The results are shown in figure 2. For the structure, (a), (c) and (e), there is little difference. For the dynamics, there are clear differences: In the case of D_t polydispersity, (b), the long-time dynamics is the same, while the short-time dynamics is fastest for the largest D_t particles. For D_r polydispersity the opposite is observed; here the short-time dynamics is the same for small and large D_r particles while the long-time dynamics is fastest for the particles with small D_r. The rotational diffusion coefficient determines a particle's persistence time because a decrease of D_r implies an increase of the long-time diffusion coefficient. Thus our observations are consistent with the single-particle scaling of the long-time diffusion coefficient. On the short time scale little change of direction is possible, making the value of D_r irrelevant.

Consider finally the case of v_0 polydispersity, (f). Here there is no effect on the short-time dynamics, while the long-time dynamics is fastest for particles with large v_0. That the short-time dynamics is unaffected is a simple consequence of equation (2) in which the v_0 term on the short time scale gives rise to a MSD proportional to t^2, which is much smaller than the short-time diffusive contribution to the MSD. The faster long-time diffusive dynamics for the large v_0 particles comes about because a larger swim velocity implies larger displacements in one direction before the direction changes,

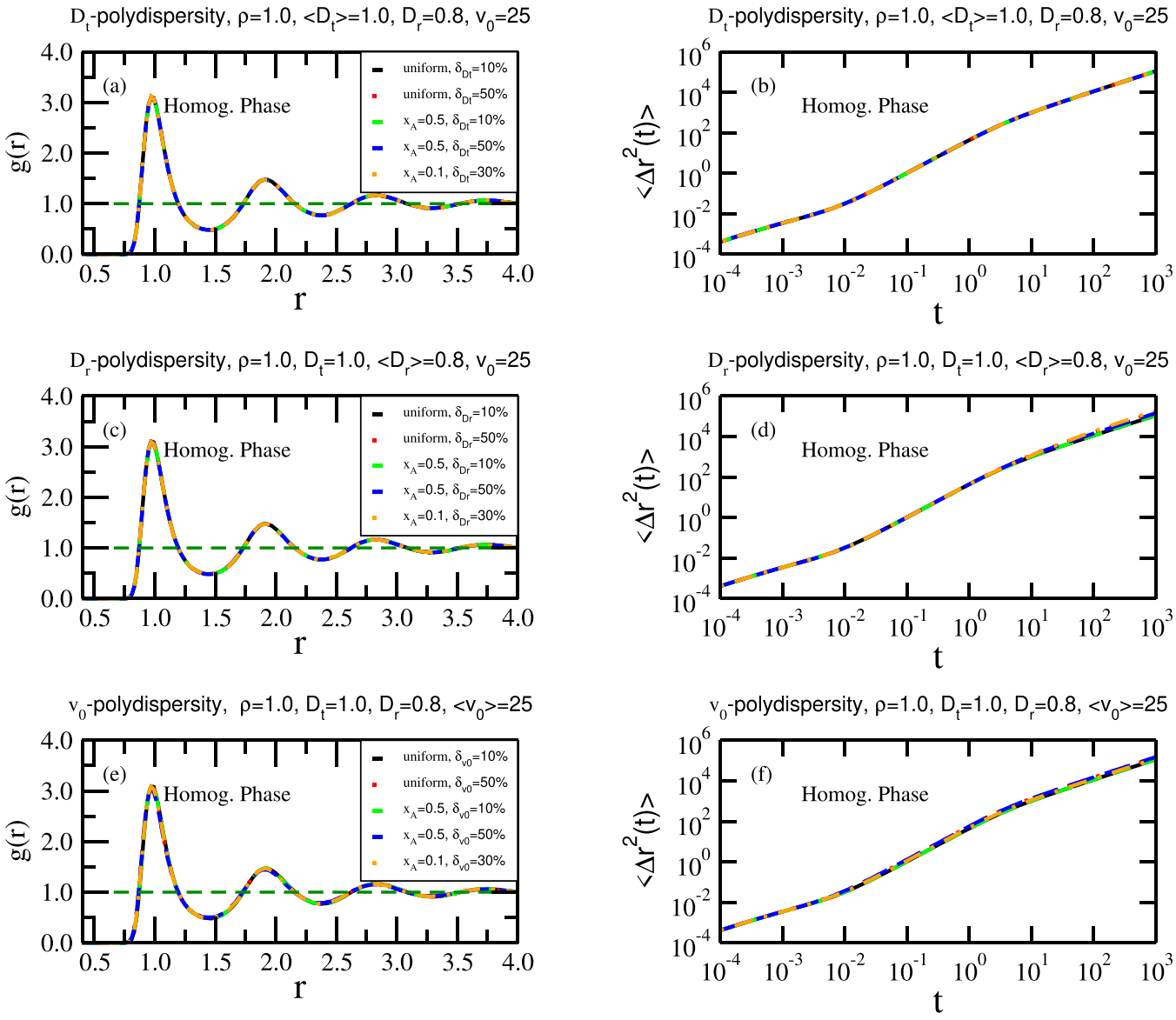

Figure 1. Structure and dynamics in the homogeneous phase for uniformly polydisperse systems (black and red curves are for 10% and 50% polydispersity) and for binary systems in which x_A is the fraction of large-parameter particles (green represents 10%, orange 30% and blue 50% polydispersity). (a), (c) and (e) show the average radial distribution functions (RDFs), $g(r)$, for systems with polydispersity in the D_t, D_r and v_0 parameters, respectively. (b), (d) and (f) show the corresponding results for the average mean-square displacement, MSD, as a function of time, $\langle \Delta r^2(t) \rangle$. In all cases there is little effect of polydispersity.

corresponding to longer jumps in a simple random-walk picture.

How do the results of figure 2 relate to the overall average structure and dynamics findings of figure 1? The structure is almost the same for small and large active parameter particles for all three types of polydispersity—and independent of the degree of polydispersity—so in this light the RDF findings of figure 1 are not surprising. In regard to the MSD, however, the variations induced by parameter polydispersity are significant but strikingly average out, resulting in little overall change of the average MSD. Thus in all three cases the black and green curves in figure 2, which represent just 10% polydispersity, are close to each other, while the red and blue curves (50% polydispersity) move in opposite directions.

4. Polydispersity in the MIPS phase

The existence of a MIPS phase is a unique feature of active matter, and MIPS is also found in the ABP model [32–34]. This phase is of interest to investigate in regard to the effects of introducing active-parameter polydispersity. We did this by repeating the simulations, the only difference being that the average of D_r is now 0.2 instead of the above used 0.8. The majority of particles are found in the dense phase at all the MIPS state points studied, implying that data found by averaging over all particles are representative for this phase.

The results for the RDFs and MSDs are shown in figure 3. In regard to the dynamics, the picture is not much different from that of the homogeneous phase: the (average) MSD is

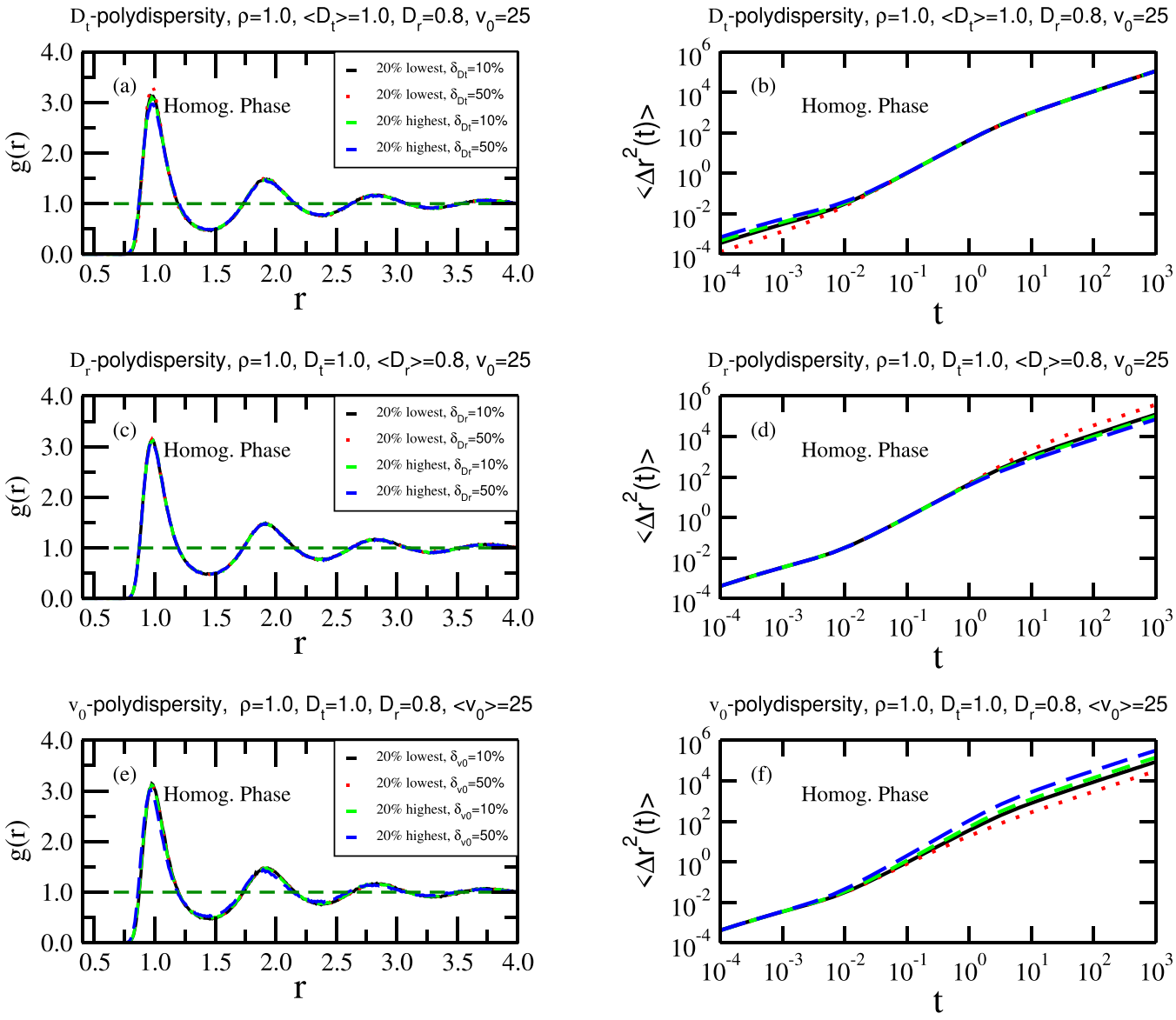

Figure 2. Role of the 20% smallest (black and red) and 20% largest (green and blue) active-parameter particles in the homogeneous phase of continuously polydisperse systems at 10% and 50% polydispersity. (a), (c) and (e) show RDFs, $g(r)$, for polydispersity in the D_t, D_r and v_0 parameter, respectively. (b), (d) and (f) show the corresponding results for the MSD, $\langle \Delta r^2(t) \rangle$. For the RDFs there is generally litte difference between the smallest and largest active-parameter particles, while the MSDs show variations that are much larger than those of the overall average (figure 1). This variation is seen in the short-time data in the case of D_t polydispersity and in the long-time data for D_r and v_0 polydispersity.

virtually unaffected by the introduction of polydispersity in the three parameters, (b), (d) and (f). The same applies for the (average) RDF for D_t and D_r polydispersity, whereas v_0 polydispersity strongly affects the RDF, (e). Note that the RDF at large r is systematically slightly larger than unity; this is an effect of the fact that the figures report the RDF averaged over all particles. While not clearly visible, a close inspection reveals that the green RDF and MSD curves cover a black one; the blue curves likewise cover a red one. The former are for 10% polydispersity in the uniform and binary cases, respectively, while the latter are for 50% polydispersity. We conclude that the introduction of v_0 polydispersity strongly affects the RDF in a way that is independent of the parameter probability distribution. Given that the existence of the MIPS phase reflects the active-matter feature of a temporary persistence direction in the particle motion, it is not surprising that introducing v_0 polydispersity has a strong effect on the structure of the MIPS phase.

To throw more light on these findings, following the procedure of the homogeneous-phase investigation we identify in figure 4 the contributions to structure and dynamics from the smallest (black and red) and largest (green and blue) parameter particles. Compared to the homogeneous case, there is more variation for all three RDFs, in particular for D_r and v_0 polydispersity. In the D_r case, the black and green curves (10% polydispersity) are close and move in the same direction when increasing to 50% polydispersity. Interestingly, the average of black and green, as well as of red and blue, is an

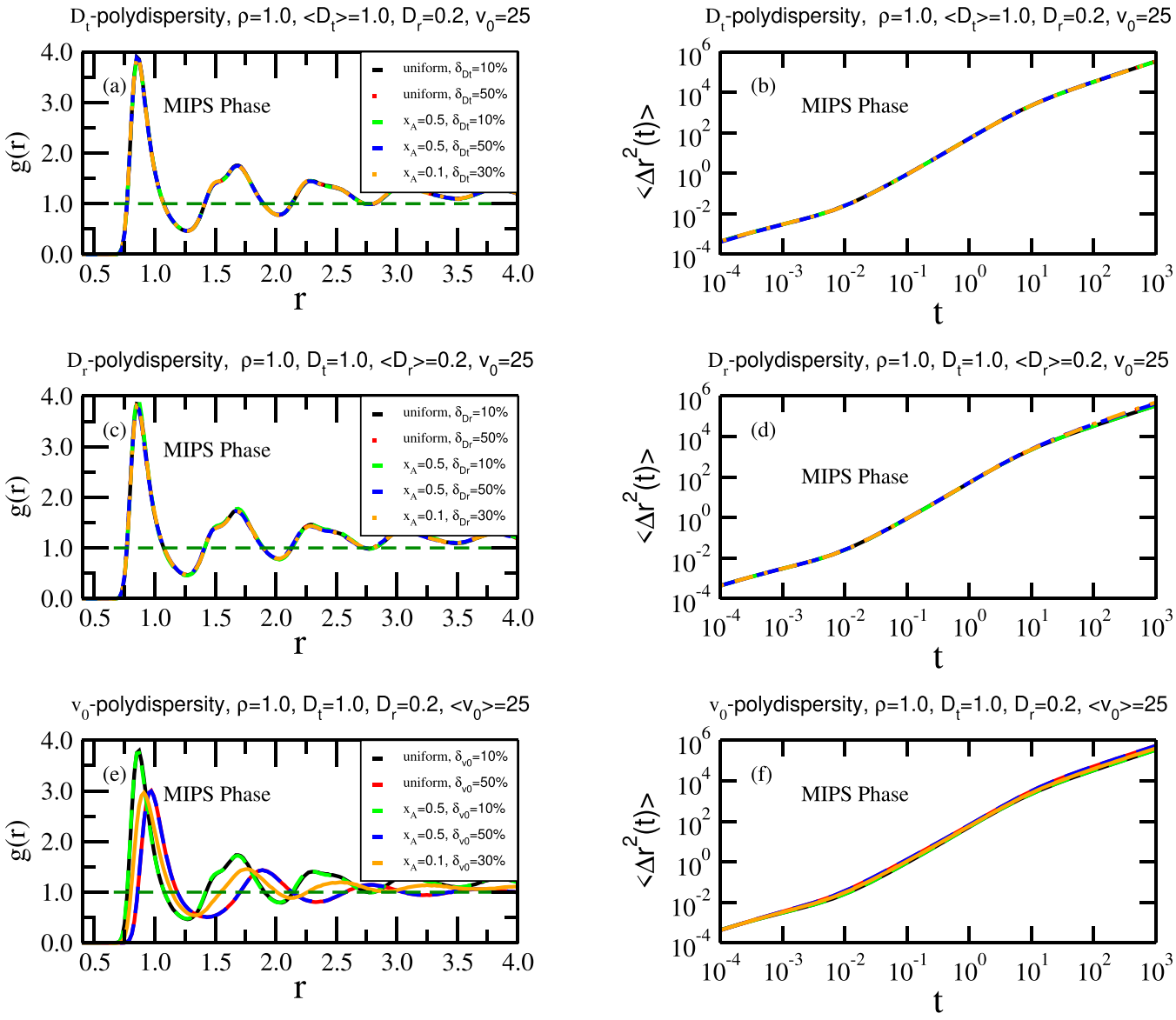

Figure 3. Structure and dynamics in the MIPS for uniformly polydisperse systems (black and red curves are for 10% and 50% polydispersity) and for binary systems in which x_A is the fraction of large-parameter particles (green represents 10%, orange 30% and blue 50% polydispersity). (a), (c) and (e) show the average RDFs for systems with polydispersity in the D_t, D_r and v_0 parameters, respectively. (b), (d) and (f) show the corresponding results for the average MSD as a function of time. There is little effect of introducing polydispersity in the D_t and D_r parameters whereas a notable effect of v_0 polydispersity is observed for the RDF, in which case there is also a visible—though much smaller—effect on the dynamics.

almost unchanged RDF, figure 3(c). The v_0 polydispersity case is different: here the 10% polydispersity curves are similar (black and green), but quite different from the 50% polydispersity curves (red and blue). This is consistent with the finding of figure 3(e) and means that the actual value of v_0 matters little for the structure surrounding a given particle. This may be caused by the strong interparticle interactions within the MIPS phase that average out the effect of the individually varying v_0. At the same time, increasing the degree of v_0 polydispersity leads to a considerable broadening of the width of the first peak. Because there is little difference between the small and large v_0 RDFs, the picture is very similar to the overall average picture. In fact, at 50% v_0 polydispersity we find that the system becomes almost homogeneous. – In regard to the MSD, the MIPS phase small- and large-parameter findings are similar to those of the homogeneous phase (figure 2).

5. Role of the average potential energy

To further illuminate the effect of parameter polydispersity we evaluated the potential energy as a function of time during the simulations (figure 5). In the homogeneous phase, (a), (c) and (e), polydispersity has little effect on the average potential energy. This is consistent with the finding that structure and dynamics are virtually unaffected by the degree of polydispersity (figure 1). The same applies for the MIPS phase in the D_t and D_r polydispersity cases. Only in the v_0-polydispersity

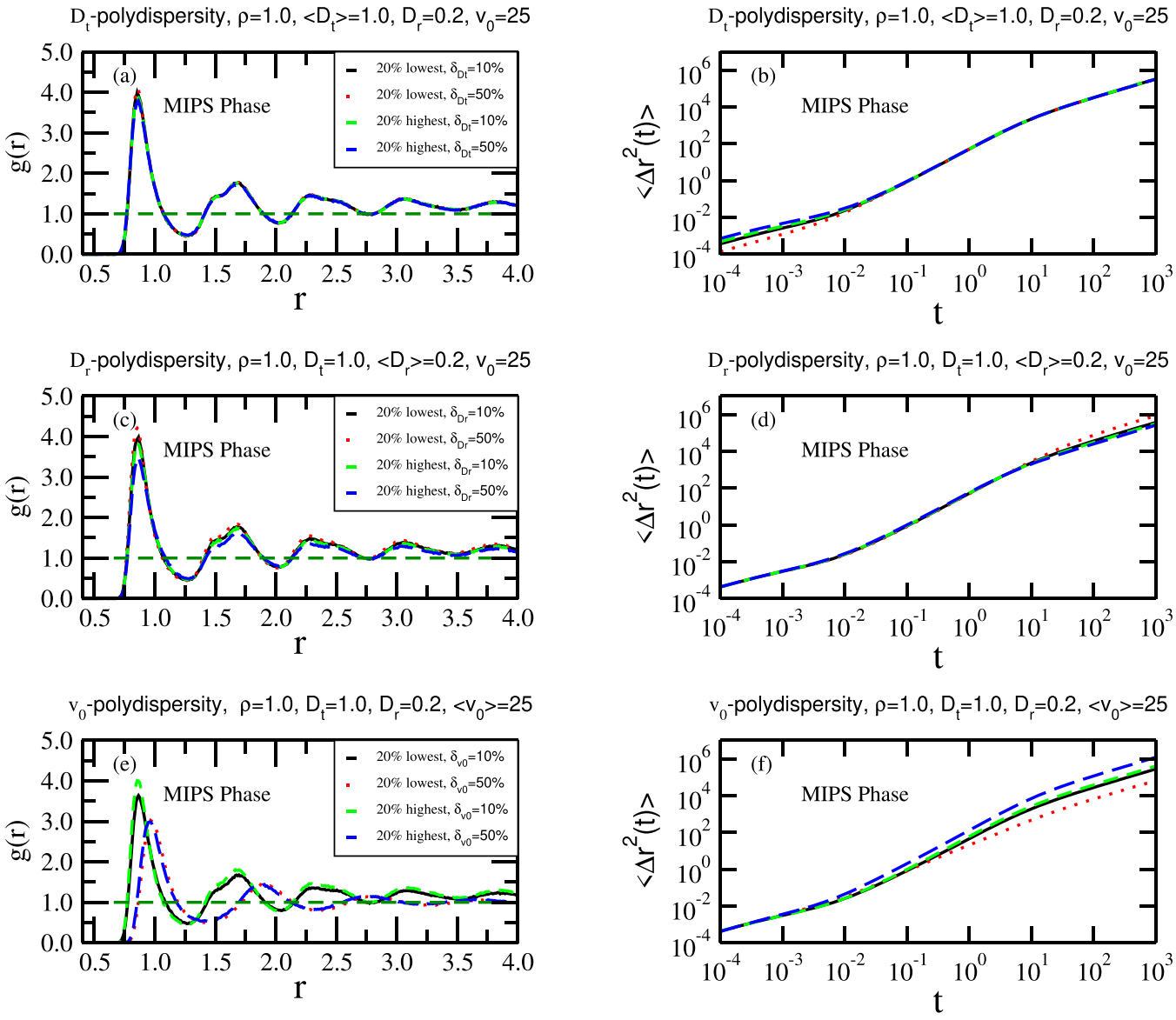

Figure 4. Role of the 20% smallest (black and red) and 20% largest (green and blue) active-parameter particles in the MIPS phase of continuously polydisperse systems at 10% and 50% polydispersity. (a), (c) and (e) show the RDFs for polydispersity in the D_t, D_r and v_0 parameters, respectively. (b), (d) and (f) show the corresponding results for the MSD. For the RDFs there is for D_t polydispersity little difference between the smallest and largest active-parameter particles except at the first peak; D_r polydispersity shows a larger but still modest difference, which is most pronounced at 50% polydispersity. The case of v_0 polydispersity shows significant differences between 10% and 50% polydispersity, but for each of these values there is only modest variation between the smallest and largest active-parameter particles' RDF. For the MSD the situation is similar to that observed in the homogeneous phase (figure 2): variation is observed in the short-time data for D_t polydispersity, in the long-time data for D_r polydispersity, and at intermediate and long times for v_0 polydispersity.

MIPS case is the structure significantly affected, figure 3(e), which is consistent with the finding that only in this case does the average potential energy change significantly with the degree of polydispersity, figure 5(f). At increasing v_0 polydispersity the MIPS-phase average potential energy approaches that of the homogeneous phase, which means that the average particle distance increases with increasing v_0 polydispersity. Indeed, in this case the position of the first peak of the RDF was found to increase toward unity, figure 3(e), indicating that the MIPS phase gradually fills out the sample area.

In summary, changes in the average potential energy upon introduction of parameter polydispersity correlate with changes of structure and dynamics. This means that the average potential energy is a convenient 'thermometer' of changes to the physics.

6. Discussion

It is well known that introducing size polydispersity into active-matter models by varying the characteristic length of the pair potential has a significant effect on both structure and dynamics [17–20, 35], just as for passive systems [29, 36, 37]. This paper investigated the effects of introducing

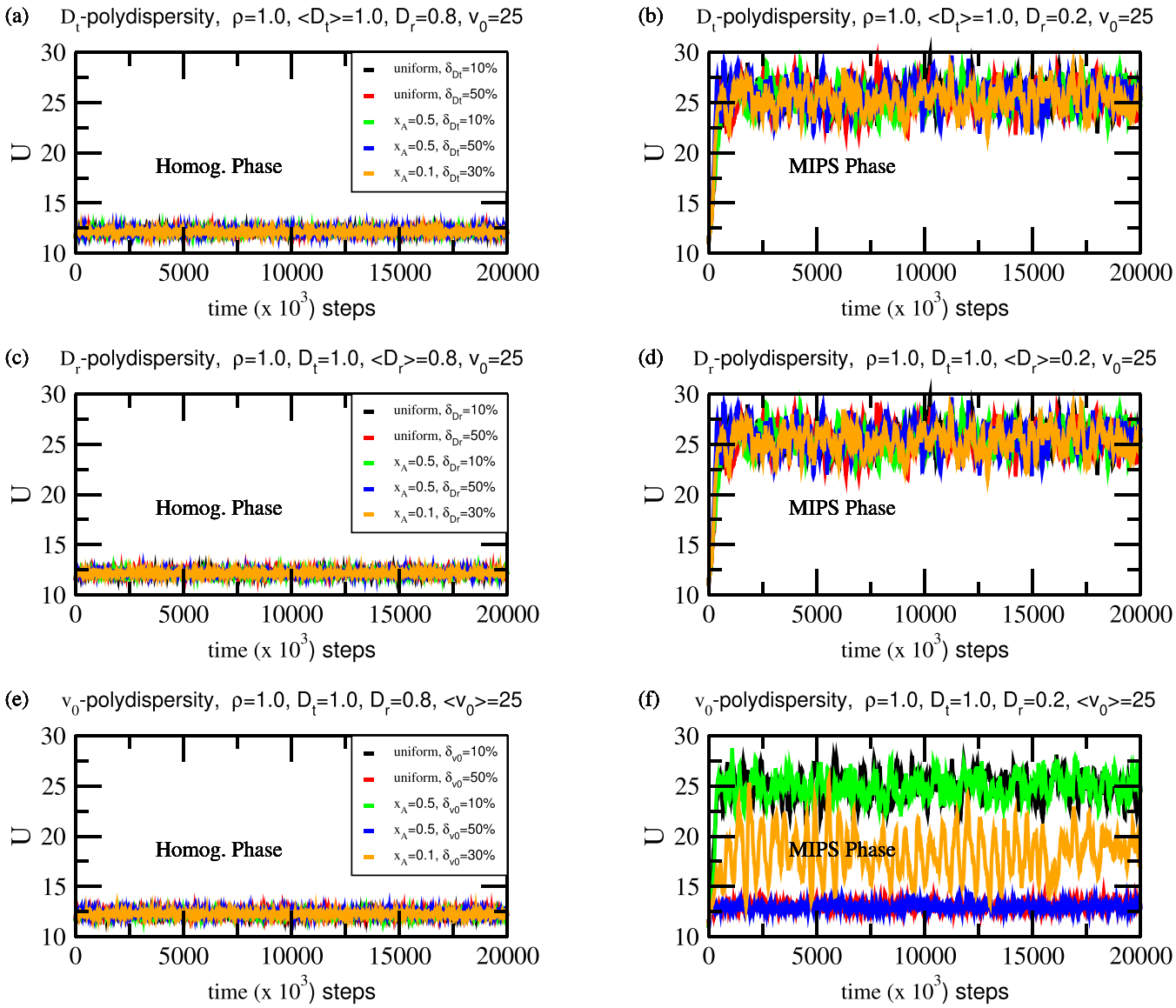

Figure 5. Average potential energy, U, as a function of time during a steady-state simulations. (a), (c) and (e) show data for the homogeneous phase for systems of 10%, 30%, and 50% polydispersity in the D_t, D_r and v_0 parameters, respectively. (b), (d) and (f) show the corresponding results for the MIPS-phase simulations. Except for the MIPS-phase v_0-polydispersity case, the average potential energy is virtually unaffected by the introduction of polydispersity.

particle-to-particle variations of other parameters of the 2d ABP model with Yukawa pair interactions. With the exception of v_0 polydispersity in the MIPS phase, we find surprisingly small effects on the structure and dynamics when polydispersity is introduced such that the average of the parameter in question is kept constant. The cause of this insensitivity to parameter polydispersity is not obvious. It means that a polydisperse active system in many respects behaves like a homogeneous system of particles with average model parameters, i.e. that a mean-field description applies to a good approximation.

While it is easy to understand the significant effects of size polydispersity [17–20, 35], we have no physical explanation for the absence of any role of polydispersity in the translational and rotational noise terms, as well as the swim velocity parameter in the homogeneous phase. It often happens in physics that a mean-field description works better than can be justified by simple arguments, and we conclude that this is indeed the case also for parameter polydispersity in active matter. We note that a recent study of Lennard–Jones (passive) systems demonstrated a similar insensitivity to the introduction of energy polydispersity [38], a result that is also not well understood.

Investigations of other active-matter models should be carried out to determine the generality of our findings. If they are general, the introduction of polydispersity may have applications to instances of non-polydisperse active-matter models for which the system in question is difficult to equilibrate because of extremely long relaxation times [39, 40]. The idea is to employ 'activity-induced annealing' [41] for a polydisperse system. As is well known, passive glass-forming polydisperse liquids may be equilibrated efficiently by the SWAP algorithm

[13]. Even though detailed balance does not apply for active matter, SWAP may possibly be applied also for equilibrating an active, single-component highly viscous system [42] by proceeding as follows. First, introduce polydispersity into one of the active-model parameters. Then, carry out random particle swaps which according to the above findings will not significantly affect the average structure and dynamics of the system. Finally, remove the artificial polydispersity. Inspired by [13] we conjecture that this procedure will equilibrate the system more quickly than a lengthy simulation.

Data availability statement

All data that support the findings of this study are included within the article (and any supplementary files).

Acknowledgments

This work was supported by the VILLUM Foundation's *Matter* Grant (VIL16515).

ORCID iDs

Shibu Saw https://orcid.org/0000-0002-6010-2477
Lorenzo Costigliola https://orcid.org/0000-0002-3324-2693
Jeppe C Dyre https://orcid.org/0000-0002-0770-5690

References

[1] Angelini T E, Hannezo E, Trepat X, Marquez M, Fredberg J J and Weitz D A 2011 Glass-like dynamics of collective cell migration *Proc. Natl Acad. Sci. USA* **108** 4714
[2] Marchetti M C, Joanny J F, Ramaswamy S, Liverpool T B, Prost J, Rao M and Simha R A 2013 Hydrodynamics of soft active matter *Rev. Mod. Phys.* **85** 1143
[3] Bechinger C, Leonardo R D, Löwen H, Reichhardt C, Volpe G and Volpe G 2016 Active particles in complex and crowded environments *Rev. Mod. Phys.* **88** 045006
[4] Ramaswamy S 2017 Active matter *J. Stat. Mech.* 054002
[5] Saintillan D 2018 Rheology of active fluids *Annu. Rev. Fluid Mech.* **50** 563
[6] Shaebani M R, Wysocki A, Winkler R G, Gompper G and Rieger H 2021 Computational models for active matter *Nat. Rev. Phys.* **2** 181
[7] Bowick M J, Fakhri N, Marchetti C M and Ramaswamy S 2022 Symmetry, thermodynamics and topology in active matter *Phys. Rev.* X **12** 010501
[8] Das S K, Egorov S A, Trefz B, Virnau P and Binder K 2014 Phase behavior of active swimmers in depletants: molecular dynamics and integral equation theory *Phys. Rev. Lett.* **112** 198301
[9] Cates M E and Tailleur J 2015 Motility-induced phase separation *Annu. Rev. Condens. Matter Phys.* **6** 219
[10] Geyer D, Martin D, Tailleur J and Bartolo D 2019 Freezing a flock: motility-induced phase separation in polar active liquids *Phys. Rev.* X **9** 031043
[11] Das M, Schmidt C F and Murrell M 2020 Introduction to active matter *Soft Matter* **16** 7185
[12] Merrigan C, Ramola K, Chatterjee R, Segall N, Shokef Y and Chakraborty B 2020 Arrested states in persistent active matter: Gelation without attraction *Phys. Rev. Res.* **2** 013260
[13] Ninarello A, Berthier L and Coslovich D 2017 Models and algorithms for the next generation of glass transition studies *Phys. Rev.* X **7** 021039
[14] Abraham S E, Bhattacharrya S M and Bagchi B 2008 Energy landscape, antiplasticization and polydispersity induced crossover of heterogeneity in supercooled polydisperse liquids *Phys. Rev. Lett.* **100** 167801
[15] Zaccarelli E, Liddle S M and Poon W C K 2015 On polydispersity and the hard sphere glass transition *Soft Matter* **11** 324
[16] Pihlajamaa I, Laudicina C C L and Janssen L M C 2023 Influence of polydispersity on the relaxation mechanisms of glassy liquids *Phys. Rev. Res.* **5** 033120
[17] Ni R, Stuart M A C and Bolhuis P G 2015 Tunable long range forces mediated by self-propelled colloidal hard spheres *Phys. Rev. Lett.* **114** 018302
[18] Henkes S, Kostanjevec K, Collinson J M, Sknepnek R and Bertin E 2020 Dense active matter model of motion patterns in confluent cell monolayers *Nat. Commun.* **11** 1405
[19] Kumar S, Singh J P, Giri D and Mishra S 2021 Effect of polydispersity on the dynamics of active Brownian particles *Phys. Rev.* E **104** 024601
[20] Szamel G and Flenner E 2021 Long-ranged velocity correlations in dense systems of self-propelled particles *Europhys. Lett.* **133** 60002
[21] de Castro P, Rocha F M, Diles S, Soto R and Sollich P 2021 Diversity of self-propulsion speeds reduces motility-induced clustering in confined active matter *Soft Matter* **17** 9926
[22] Keta Y-E, Jack R L and Berthier L 2022 Disordered collective motion in dense assemblies of persistent particles *Phys. Rev. Lett.* **129** 048002
[23] Debets V E, Löwen H and Janssen L M C 2023 Glassy dynamics in chiral fluids *Phys. Rev. Lett.* **130** 058201
[24] Yukawa H 1935 On the interaction of elementary particles. I *Proc. Phys. Math. Soc. Japan* **17** 48
[25] Hansen J-P and McDonald I R 2013 *Theory of Simple Liquids: With Applications to Soft Matter* 4th edn (Academic)
[26] Meacock O J, Doostmohammadi A, Foster K R, Yeomans J M and Durham W M 2021 Bacteria solve the problem of crowding by moving slowly *Nat. Phys.* **17** 205
[27] Saw S, Costigliola L and Dyre J C 2023 Configurational temperature in active matter. II. Quantifying the deviation from thermal equilibrium *Phys. Rev.* E **107** 024610
[28] Farage T, Krinninger P and Brader J M 2015 Effective interactions in active Brownian suspensions *Phys. Rev.* E **91** 042310
[29] Frenkel D, Vos R J, Kruif C G d and Vrij A 1986 Structure factors of polydisperse systems of hard spheres: a comparison of Monte Carlo simulations and Percus–Yevick theory *J. Chem. Phys.* **84** 4625
[30] Bailey N P *et al* 2017 RUMD: a general purpose molecular dynamics package optimized to utilize GPU hardware down to a few thousand particles *SciPost Phys.* **3** 038
[31] Caprini L and Marconi U M B 2021 Inertial self-propelled particles *J. Chem. Phys.* **154** 024902
[32] Digregorio P, Levis D, Suma A, Cugliandolo L F, Gonnella G and Pagonabarraga I 2018 Full phase diagram of active Brownian disks: from melting to motility-induced phase separation *Phys. Rev. Lett.* **121** 098003
[33] Caprini L, Marconi U M B and Puglisi A 2020 Spontaneous velocity alignment in motility-induced phase separation *Phys. Rev. Lett.* **124** 078001
[34] Caporusso C B, Digregorio P, Levis D, Cugliandolo L F and Gonnella G 2020 Motility-induced microphase and macrophase separation in a two-dimensional active Brownian particle system *Phys. Rev. Lett.* **125** 178004

[35] Jespersen D, Costigliola L, Dyre J C and Saw S 2023 Active-matter isomorphs in the size-polydisperse Ornstein–Uhlenbeck Lennard–Jones model *J. Phys.: Condens. Matter* **35** 445101
[36] Sollich P 2001 Predicting phase equilibria in polydisperse systems *J. Phys.: Condens. Matter* **14** R79
[37] Ingebrigtsen T S and Tanaka H 2015 Effect of size polydispersity on the nature of Lennard-Jones liquids *J. Phys. Chem.* B **119** 11052
[38] Ingebrigtsen T S and Dyre J C 2023 Even strong energy polydispersity does not affect the average structure and dynamics of simple liquids *J. Phys. Chem.* B **127** 2837
[39] Mandal R and Sollich P 2020 Multiple types of aging in active glasses *Phys. Rev. Lett.* **125** 218001
[40] Janzen G and Janssen L M C 2022 Aging in thermal active glasses *Phys. Rev. Res.* **4** L012038
[41] Sharma R and Karmakar S 2023 Activity-induced annealing leads to ductile-to-brittle transition in amorphous solids (arXiv:2305.17545)
[42] Paoluzzi M, Levis D and Pagonabarraga I 2022 From motility-induced phase-separation to glassiness in dense active matter *Commun. Phys.* **5** 111